# Fisher information under decoherence in Bloch representation

Wei Zhong,[1,2] Zhe Sun,[1,3] Jian Ma,[1,2] Xiaoguang Wang,[1,2,*] and Franco Nori[1,4]

[1]*Advanced Science Institute, RIKEN, Wako-shi, Saitama 351-0198, Japan*
[2]*Zhejiang Institute of Modern Physics, Department of Physics, Zhejiang University, Hangzhou 310027, China*
[3]*Department of Physics, Hangzhou Normal University, Hangzhou 310036, China*
[4]*Physics Department, The University of Michigan, Ann Arbor, Michigan 48109-1040, USA*

The dynamics of two variants of quantum Fisher information under decoherence is investigated from a geometrical point of view. We first derive the explicit formulas of these two quantities for a single qubit in terms of the Bloch vector. Moreover, we obtain analytical results for them under three different decoherence channels, which are expressed as affine transformation matrices. Using the hierarchy equation method, we numerically study the dynamics of both sets of information in a dissipative model and compare the numerical results with the analytical ones obtained by applying the rotating-wave approximation. We further express the two information quantities in terms of the Bloch vector for a qudit by expanding the density matrix and Hermitian operators in a common set of generators of the Lie algebra su($d$). By calculating the dynamical quantum Fisher information, we find that the collisional dephasing significantly diminishes the precision of the phase parameter with the Ramsey interferometry.

## I. INTRODUCTION

Quantum Fisher information (QFI), which is one of the most important quantities for both quantum estimation theory and quantum information theory, has been widely studied [1–10]. In the field of quantum estimation, the main task is to determine the value of an unknown parameter labeling the quantum system, and a primary goal is to enhance the precision of the resolution [11–26]. The inverse of the QFI provides the lower bound of the error of the estimation [27,28]. Hence, how to increase the QFI becomes the key problem to be solved. Moreover, the QFI can be used to measure the statistical distinguishability on the space of the density operators in quantum information geometry [29,30]. Recently, the QFI flow was proposed as a quantitative measure of the information flow, and it provides a novel perspective on observing the non-Markovian behavior in open quantum systems [31].

There are several variants of quantum versions of Fisher information, among which the one based on the symmetric logarithmic derivative (SLD) operator has been used most widely and possesses many good properties [27,28], such as convexity, remaining invariant under the unitary evolution, and the total amount of the QFI equivalent to the summation of the QFIs of all subsystems being uncorrelated. In this paper, we also study another variant of the quantum version of the Fisher information, which is closely related with the skew information [32]. The skew information was proposed to measure the amount of information that a quantum state contains with respect to the observable which does not commute with additive conserved quantities, such as Hamiltonians and momenta [32]. It was also used to measure the quantum uncertainty [33] and quantify quantum correlations in a bipartite state in a recent work [34]. In the following, we shall show that the two QFIs formally possess many similar features [1], but they are different not only for the concrete expressions of the

definitions, but also for their applications. As was mentioned previously, the QFI based on the SLD operator is mainly applied in quantum metrology; however, the variant version of the QFI plays an important role in quantum state discrimination [35,36].

From information theory, two different QFIs characterize the content of information contained in the quantum systems. A crucial property of these two information quantities is that they decrease monotonically under the completely positive and trace-preserving (CPT) maps [1,37–39]. The monotonicity property manifests the information loss under the CPT map. As with the introduction of the QFI flow [31], can we observe the non-Markovian properties from the perspective of the other information quantities?

Here, we will address this problem by calculating these two QFIs for a single qubit and derive the explicit formulas in the Bloch representation, which greatly facilitates the computing of these two quantities. The main results in this paper are that the dynamical QFIs, in the presence of decoherence, are analytically solved. Here, the irreversible processes are modeled via three decoherence channels [8,40–42]: the phase-damping channel (PDC), the depolarizing channel (PDC), and the generalized amplitude damping channel (GADC) [43]. The analytical results for the two information quantities under those channels are obtained. We will show that the values of the two QFIs decrease monotonically with time, apart from the isolated case in which the QFI based on the SLD operator about the amplitude parameter $\theta$ remains invariant under the PDC. To further identify the behaviors of the two QFIs subject to quantum noise, we discuss a simple model of a two-level system coupled to a reservoir with a Lorentzian spectral density [44,45]. By using the hierarchy equation method [46–53], we numerically analyze the dynamics of the two QFIs, and we compare these with the analytical solutions by using the rotating-wave approximation (RWA). We further generalize the results to the qudit system. Meanwhile, we verify that they are also applicable for the $N$-qubit system with symmetry exchange. For the sake of clarity, we calculate

*xgwang@zimp.zju.edu.cn

the dynamical quantum Fisher information in the presence of collisional dephasing.

This paper is organized as follows. In Sec. II, we first review two different definitions of the QFI, and we give the explicit formulas for the QFIs for a single-qubit system. In Sec. III, we obtain the analytical results for the two quantities under three different decoherence channels, and the numerical results are given. Moreover, in Sec. IV A, we generalize the expressions of the two QFIs for a qudit system, and the QFI in a noisy environment for an $N$-qubit system is discussed in Sec. IV B. Finally, the conclusions are given in Sec. V.

## II. FISHER INFORMATION

In this section, we briefly summarize two variants of the definition of the QFIs [32,54], which are referred to as two different extensions from the classical Fisher information. We also discuss the relations between the QFI and the Bures distance [30,55–57] as well as the QFI and the Hellinger distance [58]. In the Bloch representation, we derive the explicit formulas of these two information quantities for the single-qubit system.

### A. Fisher information and Bures distance

The classical Fisher information, originating from the statistical inference, is a way of measuring the amount of information that an observable random variable $X$ carries about an unknown parameter $\lambda$. Suppose that $\{p_i(\lambda), \lambda \in \mathbb{R}\}_{i=1}^N$ is the probability density conditioned on the fixed value of the parameter $\lambda = \lambda^*$ with measurement outcomes $\{x_i\}$. The classical Fisher information is defined as

$$F_\lambda = \sum_i p_i(\lambda) \left[ \frac{\partial \ln p_i(\lambda)}{\partial \lambda} \right]^2, \tag{1}$$

which characterizes the inverse variance of the asymptotic normality of a maximum-likelihood estimator. Here we have assumed that the observable $\hat{X}$ is a discrete variable. If it is continuous, the summation in Eq. (1) should be replaced by an integral.

The quantum analog of the Fisher information is formally generalized from Eq. (1) and defined as

$$\mathcal{F}_\lambda = \text{Tr}\left( \rho_\lambda L_\lambda^2 \right) = \text{Tr}\left[ (\partial_\lambda \rho_\lambda) L_\lambda \right], \tag{2}$$

in terms of the symmetric logarithmic derivative (SLD) operator $L_\lambda$, which is a Hermitian operator determined by

$$\partial_\lambda \rho_\lambda = \frac{1}{2}\{\rho_\lambda, L_\lambda\}, \tag{3}$$

where $\partial_\lambda \equiv \frac{\partial}{\partial \lambda}$ and $\{\cdot, \cdot\}$ denotes the anticommutator. By diagonalizing the density matrix as $\rho_\lambda = \sum_i \varrho_i |\psi_i\rangle \langle\psi_i|$, associated with $\varrho_i \geqslant 0$ and $\sum_i \varrho_i = 1$, the elements of the SLD operator are completely defined under the condition $\varrho_i + \varrho_j \neq 0$. Therefore, Eq. (2) can be expressed as

$$\mathcal{F}_\lambda = \sum_{i'} \frac{(\partial_\lambda \varrho_{i'})^2}{\varrho_{i'}} + 2 \sum_{i \neq j} \frac{(\varrho_i - \varrho_j)^2}{\varrho_i + \varrho_j} |\langle\psi_i|\partial_\lambda \psi_j\rangle|^2, \tag{4}$$

where the first and the second summations involve sums over all $\varrho_{i'} \neq 0$ and $\varrho_i + \varrho_j \neq 0$, respectively. In Eq. (4), the first term is equal to the classical Fisher information of Eq. (2),

which is called the classical term, and the second term is called the quantum term. For pure states, Eq. (4) reduces to

$$\mathcal{F}_\lambda = 4[\langle\partial_\lambda \psi|\partial_\lambda \psi\rangle - |\langle\psi|\partial_\lambda \psi\rangle|^2]. \tag{5}$$

An essential feature of the QFI is that we can obtain the achievable lower bound of the mean-square error of the unbiased estimator for the parameter $\lambda$, i.e., the so-called quantum Cramér-Rao (QCR) theorem:

$$\text{var}(\hat{\lambda}) \geqslant \frac{1}{\nu \mathcal{F}_\lambda}, \tag{6}$$

where $\text{var}(\cdot)$ denotes the variance, $\hat{\lambda}$ denotes the unbiased estimator, and $\nu$ represents the number of repeated experiments. It has been found that the QCR bound cannot be achieved in the asymptotic limit, and other measures of the accuracy are examined in Refs. [24–26].

As shown in a seminal work, see Ref. [30], the estimability of a set of parameters parametrizing the family of the quantum states $\{\rho_\lambda\}$, which is characterized by the QFI, is naturally related to the distinguishability of the states on the manifold of the quantum states, which is measured by the Bures distance. It was also proven that the QFI is simply proportional to the Bures distance [30],

$$D_B^2[\rho(\lambda), \rho(\lambda + d\lambda)] = \frac{1}{4}\mathcal{F}_\lambda \, d\lambda^2. \tag{7}$$

The Bures distance measures the distance between two quantum states, and is defined as [55–57]

$$D_B^2(\rho, \sigma) := 2(1 - \text{Tr}\sqrt{\rho^{1/2}\sigma\rho^{1/2}}), \tag{8}$$

where the second term in the parentheses on the right-hand side is the so-called Uhlmann fidelity [56]. Meanwhile, the explicit formula of the QFI for the two-dimensional density matrices is obtained by Ref. [59]

$$\mathcal{F}_\lambda = \text{Tr}(\partial_\lambda \rho)^2 + \frac{1}{\det\rho}\text{Tr}(\rho \, \partial_\lambda \rho)^2. \tag{9}$$

In the Bloch sphere representation, any qubit state can be written as

$$\rho = \frac{1}{2}(\mathbb{1} + \boldsymbol{\omega} \cdot \hat{\boldsymbol{\sigma}}), \tag{10}$$

where $\boldsymbol{\omega} = (\omega_x, \omega_y, \omega_z)^\mathsf{T}$ is the real Bloch vector and $\hat{\boldsymbol{\sigma}} = (\hat{\sigma}_x, \hat{\sigma}_y, \hat{\sigma}_z)$ denotes the Pauli matrices. Apparently, the eigenvalues of the density operator are $(1 \pm \omega)/2$, with the length of the Bloch vector $\omega \equiv |\boldsymbol{\omega}|$. Here, the Bloch vector satisfies $\omega \leqslant 1$, and the equality holds for pure states. In the Bloch representation, $\mathcal{F}_\lambda$ can be represented as follows:

$$\mathcal{F}_\lambda = \begin{cases} |\partial_\lambda \boldsymbol{\omega}|^2 + \frac{(\boldsymbol{\omega} \cdot \partial_\lambda \boldsymbol{\omega})^2}{1 - |\boldsymbol{\omega}|^2}, & \omega < 1, \\ |\partial_\lambda \boldsymbol{\omega}|^2, & \omega = 1. \end{cases} \tag{11}$$

The first line of the above equation is only applicable for the mixed states, which can be straightforwardly obtained by substituting Eq. (10) into Eq. (9).

For pure states, we have the equation $\rho^2 = \rho$. Taking the differential on both sides of this equation with respect to $\lambda$, one gets

$$\partial_\lambda \rho = \partial_\lambda \rho^2 = \rho(\partial_\lambda \rho) + (\partial_\lambda \rho)\rho. \tag{12}$$

The SLD operator is given as

$$L = 2\,\partial_\lambda \rho \tag{13}$$

by comparing Eq. (12) with Eq. (3). Substituting Eqs. (10) and (13) into Eq. (2), and using the relation

$$\mathrm{Tr}\left[(\boldsymbol{a}\cdot\hat{\boldsymbol{\sigma}})(\boldsymbol{b}\cdot\hat{\boldsymbol{\sigma}})\right]=2\,\boldsymbol{a}\cdot\boldsymbol{b}, \tag{14}$$

finally yields the second line of Eq. (11), i.e., $\mathcal{F}_\lambda$ for pure states is the norm of the derivative of the Bloch vector.

### B. Fisher information and Hellinger distance

By extending Eq. (1) into the quantum regime in a different way, we will obtain a variant QFI [60]. Equation (1) can be equivalently expressed as

$$F_\lambda=4\sum_i[\partial_\lambda\sqrt{p_i(\lambda)}]^2. \tag{15}$$

By straightforwardly replacing the summation by a trace, the probability $p_i(\lambda)$ by a density matrix $\rho_\lambda$, and the differential $\partial_\lambda$ by the inner differential $\partial_\lambda\cdot\equiv i[\hat{G},\cdot]$ with $\hat{G}$ being a fixed self-adjoint operator and $[\cdot,\cdot]$ denoting the commutator, one obtains the following equation:

$$\mathcal{I}_\lambda:=4\mathrm{Tr}(\partial_\lambda\sqrt{\rho}_\lambda)^2=-4\mathrm{Tr}\big[\rho^{1/2},\hat{G}\big]^2. \tag{16}$$

In this particular case, suppose that $\rho_\lambda\equiv e^{-i\hat{G}\lambda}\rho e^{i\hat{G}\lambda}$, i.e., $\rho_\lambda$ satisfies the Landau–von Neumann equation $i\partial_\lambda\rho_\lambda=[\hat{G},\rho_\lambda]$. Note that here we define Eq. (16) as a paradigmatic version of the QFI. Actually, Eq. (16) is the so-called skew information

$$\mathcal{I}_{\mathrm{WY}}:=-\tfrac{1}{2}\mathrm{Tr}\big[\rho_\lambda^{1/2},\hat{G}\big]^2, \tag{17}$$

which is introduced by Wigner and Yanase [32], with ignorance of a negligible constant number here, i.e., $\mathcal{I}=8\mathcal{I}_{\mathrm{WY}}$. The skew information (SI) is a measure of the information contained in a quantum state $\rho_\lambda$ with respect of a fixed conserved observable $\hat{G}$.

By inserting the spectrum decomposition $\rho=\sum_i\varrho_i|\psi_i\rangle\langle\psi_i|$ into Eq. (16), one obtain

$$\mathcal{I}_\lambda=\sum_{i'}\frac{(\partial_\lambda\varrho_{i'})^2}{\varrho_{i'}}+4\sum_{i\neq j}(\sqrt{\varrho_i}-\sqrt{\varrho_j})^2|\langle\psi_i|\partial_\lambda\psi_j\rangle|^2, \tag{18}$$

where the first summation is over all $\varrho_i\neq 0$, the same requirement as in Eq. (18). Comparing with Eq. (4), the classical terms in Eqs. (4) and (18) are the same, but the quantum terms are different. For pure states, Eq. (18) reduces to

$$\mathcal{I}_\lambda=8[\langle\partial_\lambda\psi|\partial_\lambda\psi\rangle-|\langle\psi|\partial_\lambda\psi\rangle|^2], \tag{19}$$

which is twice as much as the QFI of Eq. (2) given in Eq. (5). The factor-of-2 difference between $\mathcal{F}_\lambda$ and $\mathcal{I}_\lambda$ results from their different coefficients (or weights) of the quantum terms in Eqs. (4) and (18). For pure states, the classical terms vanish, and only the quantum terms contribute. Then we obtain Eqs. (5) and (19).

Similar to the relation between the QFI of Eq. (2) and the Bures distance given in Eq. (7), there formally exists the same relation between the QFI of Eq. (17) and the quantum Hellinger distance [58]:

$$D^2_{\mathrm{QH}}[\rho(\lambda),\rho(\lambda+d\lambda)]=\tfrac{1}{4}\mathcal{I}_\lambda\,d\lambda^2. \tag{20}$$

The latter is the quantum version of the classical Hellinger distance, which measures the distance between two probability distributions. In the space of the quantum state, the quantum Hellinger distance is defined as

$$D^2_{\mathrm{QH}}(\rho,\sigma):=2(1-\mathrm{Tr}\sqrt{\rho}\sqrt{\sigma}), \tag{21}$$

where the last term in the parentheses on the right-hand side is called quantum affinity [58].

For a $2\times 2$ density matrix, we derive the explicit formula of the QFI $\mathcal{I}_\lambda$ as follows:

$$\mathcal{I}_\lambda=\alpha\,\mathrm{Tr}(\partial_\lambda\rho)^2-\beta\,\mathrm{Tr}(\rho\,\partial_\lambda\rho)^2, \tag{22}$$

where the coefficients are determined by

$$\alpha=\frac{1}{1-4\det\rho}\left[\frac{4(1-2\det\rho)}{(1+2\sqrt{\det\rho})}-1\right], \tag{23}$$

$$\beta=\frac{1}{1-4\det\rho}\left(\frac{8}{1+2\sqrt{\det\rho}}-\frac{1}{\det\rho}\right). \tag{24}$$

In the Bloch representation, $\mathcal{I}_\lambda$ can be represented as follows:

$$\mathcal{I}_\lambda=\begin{cases}\frac{2|\partial_\lambda\boldsymbol{\omega}|^2}{1+\sqrt{1-|\boldsymbol{\omega}|^2}}+\Theta_{\boldsymbol{\omega}}\,(\boldsymbol{\omega}\cdot\partial_\lambda\boldsymbol{\omega})^2, & \omega<1,\\ 2\,|\partial_\lambda\boldsymbol{\omega}|^2, & \omega=1,\end{cases} \tag{25}$$

where the coefficient is given by

$$\Theta_{\boldsymbol{\omega}}=\frac{1}{1-|\boldsymbol{\omega}|^2}-\frac{1}{(1+\sqrt{1-|\boldsymbol{\omega}|^2})^2}. \tag{26}$$

The first line of Eq. (25) is only applicable for mixed states, which can be directly derived by substituting Eq. (10) into Eqs. (22), (23), and (24).

For pure states, we have

$$\sqrt{\rho}=\rho. \tag{27}$$

With Eqs. (14) and (27), one can obtain the second line of Eq. (25) from Eq. (16), i.e., $\mathcal{I}_\lambda$ for pure states is the norm of the derivative of the Bloch vector up to a factor of 2.

### C. Example

Having obtained Eqs. (11) and (25), we consider a simple example to calculate the two variant QFIs for a pure state with different parameters. We adopt the standard notation where $|1\rangle\equiv|\downarrow\rangle$ and $|0\rangle\equiv|\uparrow\rangle$ correspond to the ground state and excited state, respectively. Consider an arbitrary single-qubit state

$$|\psi\rangle=\cos\frac{\theta}{2}|0\rangle+e^{i\phi}\sin\frac{\theta}{2}|1\rangle, \tag{28}$$

of which the Bloch vector is denoted as $\boldsymbol{\omega}=(\sin\theta\cos\phi,\ \sin\theta\sin\phi,\ \cos\theta)^{\mathrm{T}}$, with $\theta$ and $\phi$ referring to the polar and azimuth angles on the Bloch sphere. Here, the two parameters $\theta$ and $\phi$ in Eq. (28) are assumed to be unitary encoded.

Now we compute the QFIs of the single-qubit state Eq. (28) in terms of the following parameters: $\theta$ (amplitude parameter) and $\phi$ (phase parameter). With the help of Eq. (11), one can easily obtain $\mathcal{F}_\theta=1$ and $\mathcal{F}_\phi=\sin^2\theta$. For the amplitude parameter $\theta$, $\mathcal{F}_\theta$ is constantly equal to 1, independent of both parameters $\theta$ and $\phi$, while $\mathcal{F}_\phi$ about $\phi$ depends on the parameter $\theta$ and reaches the maximum value 1 when $\theta=\pi/2$, i.e., $|\psi\rangle$ is an equal-weighted state $|\psi\rangle=(|0\rangle+e^{i\phi}|1\rangle)/\sqrt{2}$

[11]. According to Eq. (25), we obtain $\mathcal{I}_\theta = 2$ and $\mathcal{I}_\phi = 2\sin^2\theta$. Similar to $\mathcal{F}_\theta$, $\mathcal{I}_\theta$ is also independent of the parameters $\theta$ and $\phi$. Meanwhile, $\mathcal{I}_\phi$ reaches the maximum value 2 at the point $\theta = \pi/2$. In Sec. III B, we will assume that the qubit is initially in the equally weighted superposition of the two states $|0\rangle$ and $|1\rangle$, so both $\mathcal{F}_\phi$ and $\mathcal{I}_\phi$ reach their maximum values.

## III. QFI FOR A SINGLE QUBIT UNDER DECOHERENCE

Decoherence occurs when a quantum system interacts with its environment, and it is unavoidable in almost all realistic quantum systems. A quantum noisy dynamical process can be generally described by a map $\mathcal{E}$ using the Kraus representation

$$\mathcal{E}(\rho) = \sum_\mu K_\mu \, \rho \, K_\mu^\dagger, \qquad (29)$$

where $K_\mu$ are the Kraus operators satisfying $\sum_\mu K_\mu^\dagger K_\mu = \mathbb{1}$, which leads to the map $\mathcal{E}$ being a CPT map [37,38]. In the Bloch representation, such a nonunital trace-preserving process can be represented by an affine map on the generalized Bloch vector [40,61].

For a qubit system, Eq. (29) can be equivalently represented as

$$\mathcal{E}(\rho) = \tfrac{1}{2}\mathbb{1} + \tfrac{1}{2}(A\,\boldsymbol{\omega} + \mathbf{c}) \cdot \hat{\boldsymbol{\sigma}}, \qquad (30)$$

where $A$ is a $3 \times 3$ real transformation matrix with elements defined as $A_{ij} = \tfrac{1}{2}\mathrm{Tr}[\sigma_i \mathcal{E}(\sigma_j)]$, and $\mathbf{c} \in \mathbb{R}^3$ is the translation vector with elements given by $c_i = \tfrac{1}{2}\mathrm{Tr}[\sigma_i \mathcal{E}(\mathbb{1})]$. From Eqs. (10) and (30), it indicates that under decoherence, the Bloch vector $\boldsymbol{\omega}$ of Eq. (10) is mapped as $\mathcal{E}(\boldsymbol{\omega}) := A\boldsymbol{\omega} + \mathbf{c}$. In parameter estimation, the unknown parameter is generally encoded on the probes through a unitary or nonunitary evolution [15]. In this paper, we do not consider the case of the nonunitary parametrization. $A$ and $\mathbf{c}$ are assumed to be parameter-independent, i.e., the decoherence process will not introduce the parameter.

With Eq. (11), the dynamics of the QFI based on the SLD operator for a single qubit under decoherence channels can be generally expressed as

$$\mathcal{F}_\lambda = |\partial_\lambda \mathcal{E}(\boldsymbol{\omega})|^2 + \frac{[\mathcal{E}(\boldsymbol{\omega}) \cdot \partial_\lambda \mathcal{E}(\boldsymbol{\omega})]^2}{1 - |\mathcal{E}(\boldsymbol{\omega})|^2}. \qquad (31)$$

Similarly, according to Eq. (25), the dynamics of the variant version of the QFI can be written as

$$\mathcal{I}_\lambda = \frac{2\,|\partial_\lambda \mathcal{E}(\boldsymbol{\omega})|^2}{1 + \sqrt{1 - |\mathcal{E}(\boldsymbol{\omega})|^2}} + \Theta_{\mathcal{E}(\boldsymbol{\omega})}\,[\mathcal{E}(\boldsymbol{\omega}) \cdot \partial_\lambda \mathcal{E}(\boldsymbol{\omega})]^2. \qquad (32)$$

Given an input state $|\psi\rangle$, the dynamics of the two QFIs under quantum channels is fully determined by the affine transformation matrix $A$ and the translation vector $\mathbf{c}$. It is noted that Eqs. (31) and (32) are the general results that are applicable to all of those cases with different parametrization processes.

### A. Dynamics of the QFIs under three decoherence channels

Below, we will study the dynamics of the two variant versions of the QFI under three paradigmatic types of quantum channels [40,43]: a phase-damping channel (PDC), a depolarizing channel (DPC), and a generalized amplitude-damping channel (GADC) modeling a thermal bath at arbitrary temperature, which will be reduced to a purely dissipative amplitude-damping channel (ADC) when the environment temperature becomes zero. These channels are the prototype models of dissipation relevant in various experimental systems,

#### 1. Phase-damping channel

The PDC is a prototype model of dephasing or pure decoherence, i.e., loss of coherence of a two-level state without any loss of system energy. The PDC is described by the map

$$\mathcal{E}_{\mathrm{PDC}}(\rho) = s\,\rho + p\,(\rho_{00}|0\rangle\langle0| + \rho_{11}|1\rangle\langle1|), \qquad (33)$$

and obviously the Kraus operators are given by

$$\mathbf{K}_{\mathrm{PDC}} = \{\sqrt{s}\,\mathbb{1},\ \sqrt{p}\,|0\rangle\langle0|,\ \sqrt{p}\,|1\rangle\langle1|\}, \qquad (34)$$

where $p \equiv 1 - s$ is the probability of the qubit exchanging a quantum with the bath at time $t$ with $s = \exp(-\gamma t/2)$, with $\gamma$ denoting the zero-temperature dissipation rate. For the sake of simplicity, we introduce a dimensionless quantity $\tau = \gamma t$, then $s = \exp(-\tau/2)$. For the PDC, there is no energy change and a loss of decoherence occurs with probability $p$. As a result of the action of the PDC, the Bloch sphere is compressed by a factor $(1 - 2p)$ in the $xy$ plane.

According to Eq. (30), the transformation matrix $A$ and the translation vector $\mathbf{c}$ of the PDC are given in Table I. These indicate that the Bloch vector components along the $x$ and $y$ axis shrink with probability $s$, while the $z$ component remains invariant under the action of the PDC, and the Bloch vector $\boldsymbol{\omega}$ is mapped as

$$\mathcal{E}_{\mathrm{PDC}}(\boldsymbol{\omega}) = (s\,\omega_x, s\,\omega_y, \omega_z)^{\mathrm{T}}. \qquad (35)$$

Furthermore, with Eqs. (31) and (32), we obtain the analytical results of the two variant versions of the QFI under the PDC in Table I. One can find that $\mathcal{F}_\phi$, $\mathcal{I}_\theta$, and $\mathcal{I}_\phi$ are monotonic functions of $t$ and are solely dependent on the parameter $\theta$. Interestingly, $\mathcal{F}_\theta$ is constantly equal to 1 for any time, which implies that the QFI $\mathcal{F}$ about the amplitude parameter $\theta$ is robust under PDC. The significance of this is that one can avoid the impact of the PDC on the accuracy of the parameter estimation by encoding the parameter on the amplitude of the input state.

When $\theta = \pi/2$, we have

$$\mathcal{F}_\theta = 1, \quad \mathcal{F}_\phi = s^2,$$
$$\mathcal{I}_\theta = \frac{2}{1 + \sqrt{1 - s^2}}, \quad \mathcal{I}_\phi = 2 - 2\sqrt{1 - s^2}.$$

As is plotted in Figs. 1(a) and 1(b), under the PDC, the QFIs associated with the phase parameter, $\mathcal{F}_\phi$ and $\mathcal{I}_\phi$, decreases monotonically with $\tau$ and vanish only in the asymptotic limit $\tau \to \infty$. Interestingly, $\mathcal{I}_\theta$ decreases from the initial value 2 to the final value 1, shown in Fig. 1(b). It is indicated that the QFI $\mathcal{I}_\theta$ depends on the diagonal and off-diagonal elements of the density matrix. Due to the influence of the PDC, the off-diagonal ones vanish, and only the diagonal ones remain, which makes $\mathcal{I}_\theta$ equal to 1.

TABLE I. Analytical results for the time evolutions of the two QFI quantities in terms of the parameters $\theta$ and $\phi$ for the single-qubit state $|\psi\rangle$ in Eq. (28) under the quantum decoherence channels. The decoherence channels can geometrically be described as affine maps, and the transformation matrices $A$ and the translation vectors $c$ for each channel are listed. To simplify the expression of the results, we set $X = \sin\theta\sqrt{1-s^2}$, $Y = 2\cos^2\frac{\theta}{2}\sqrt{s(1-s)}$, $Z = \sqrt{1-\bar{s}\sin^2\theta - [\bar{p}(\alpha-\beta)-\bar{s}\cos\theta]^2}$, $R_1 = \bar{s}[1+\bar{s}+\bar{p}\cos(2\theta)]$, and $R_2 = \bar{p}^2\bar{s}^2(\alpha-\beta+\cos\theta)^2\sin^2\theta$.

| Quantum channel | $A$ | $c$ | $\mathcal{F}_\theta$ | $\mathcal{F}_\phi$ | $\mathcal{I}_\theta$ | $\mathcal{I}_\phi$ |
|---|---|---|---|---|---|---|
| Phase-damping channel (PDC) | $\begin{pmatrix} s & 0 & 0 \\ 0 & s & 0 \\ 0 & 0 & 1 \end{pmatrix}$ | $\begin{pmatrix} 0 \\ 0 \\ 0 \end{pmatrix}$ | $1$ | $s^2\sin^2\theta$ | $\frac{3+4X+2s^2\cos^2\theta-\cos(2\theta)}{2(1+X)^2}$ | $\frac{2s^2\sin^2\theta}{1+X}$ |
| Depolarizing channel (DPC) | $\begin{pmatrix} s & 0 & 0 \\ 0 & s & 0 \\ 0 & 0 & s \end{pmatrix}$ | $\begin{pmatrix} 0 \\ 0 \\ 0 \end{pmatrix}$ | $s^2$ | $s^2\sin^2\theta$ | $2-2\sqrt{1-s^2}$ | $\frac{2s^2\sin^2\theta}{1+\sqrt{1-s^2}}$ |
| Amplitude damping channel (ADC) | $\begin{pmatrix} \sqrt{s} & 0 & 0 \\ 0 & \sqrt{s} & 0 \\ 0 & 0 & s \end{pmatrix}$ | $\begin{pmatrix} 0 \\ 0 \\ -p \end{pmatrix}$ | $s$ | $s\sin^2\theta$ | $\frac{s[3+4Y+2s\sin^2\theta+\cos(2\theta)]}{2(1+Y)^2}$ | $\frac{2s\sin^2\theta}{1+Y}$ |
| Generalized amplitude damping channel (GADC) | $\begin{pmatrix} \sqrt{\bar{s}} & 0 & 0 \\ 0 & \sqrt{\bar{s}} & 0 \\ 0 & 0 & \bar{s} \end{pmatrix}$ | $\begin{pmatrix} 0 \\ 0 \\ -\bar{p}(\alpha-\beta) \end{pmatrix}$ | $\frac{R_1}{2}+\frac{R_2}{Z}$ | $\bar{s}\sin^2\theta$ | $\frac{R_1}{1+Z}+R_2\left[\frac{1}{Z^2}-\frac{1}{(1+Z)^2}\right]$ | $\frac{2\bar{s}\sin^2\theta}{1+Z}$ |

## 2. Depolarizing channel

The definition of the DPC is given via the map

$$\mathcal{E}_{\mathrm{DPC}}(\rho) = s\,\rho + p\,\frac{\mathbb{1}}{2}, \tag{36}$$
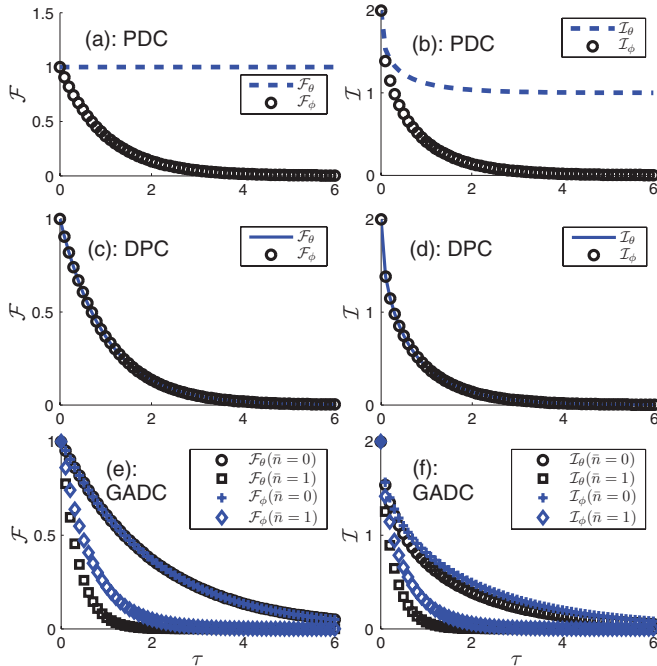


FIG. 1. (Color online) Plots of the two variant versions of the QFI vs $\tau$ in terms of the parameters $\theta$ and $\phi$ under three quantum decoherence channels: PDC (a),(b), DPC (c),(d), and GADC (e),(f) for a single-qubit system. The qubit initially being prepared is in the equally weighted state [Eq. (28) with $\theta = \pi/2$] of which the QFIs take the maximum at $\tau = 0$. In (e) and (f), we plot the QFIs under the GADC for zero temperature $\bar{n} = 0$ and finite temperature $\bar{n} = 1$, respectively.

and the corresponding Kraus operators are expressed as

$$\mathbf{K}_{\mathrm{DPC}} = \left\{ \frac{\sqrt{1+3s}}{2}\mathbb{1}, \frac{\sqrt{p}}{2}\sigma_x, \frac{\sqrt{p}}{2}\sigma_y, \frac{\sqrt{p}}{2}\sigma_z \right\}, \tag{37}$$

where $s \equiv 1 - p$ and $\boldsymbol{\sigma} = (\sigma_x, \sigma_y, \sigma_z)^{\mathrm{T}}$ denotes the Pauli matrices. The channel is completely positive for $0 \leqslant p \leqslant 1$. We see that for the DPC, the qubit is unchanged with probability $s$ or it is depolarized to the completely mixed state $\mathbb{1}/2$ with probability $p$. It is seen that due to the action of the DPC, the radius of the Bloch sphere is reduced by a factor $s$, but its shape remains unchanged.

The transformation matrix $A$ and the translation vector $c$ for the DPC are given in Table I, and then the affine-mapped Bloch vector is obtained as

$$\mathcal{E}_{\mathrm{DPC}}(\boldsymbol{\omega}) = (s\,\omega_x, s\,\omega_y, s\,\omega_z)^{\mathrm{T}}, \tag{38}$$

which shows that all components of the Bloch vector are shortened by a factor $s$. Moreover, we analytically derive the expressions of the two QFIs with respect to $\theta$ and $\phi$ under the DPC, given in Table I.

For $\theta = \pi/2$, those expressions are explicitly simplified as

$$\mathcal{F}_\theta = \mathcal{F}_\phi = s^2, \quad \mathcal{I}_\theta = \mathcal{I}_\phi = 2 - 2\sqrt{1-s^2}.$$

The results show that, under the DPC, the two QFIs decrease by a factor of $s^2$ and $s$, respectively. The expressions of the QFI $\mathcal{F}$ ($\mathcal{I}$) for different parameters $\theta$ and $\phi$ are the same. As plotted in Figs. 1(c) and 1(d), the QFIs decreases monotonically.

## 3. Generalized amplitude-damping channel

The GADC is given, in the Born-Markov approximation, via its Kraus representation as

$$\mathcal{E}_{\mathrm{GADC}}(\rho) = \sum_{i=0}^{3} K_i\,\rho\,K_i^\dagger, \tag{39}$$

where the corresponding Kraus operators are

$$\mathbf{K}_{\text{GADC}} = \{\sqrt{\alpha}(|0\rangle\langle 0| + \sqrt{\bar{s}}|1\rangle\langle 1|), \sqrt{\alpha\,\bar{p}}|0\rangle\langle 1|,$$
$$\sqrt{\beta}(\sqrt{\bar{s}}|0\rangle\langle 0| + |1\rangle\langle 1|), \sqrt{\beta\,\bar{p}}|1\rangle\langle 0|\}, \quad (40)$$

with

$$\alpha \equiv \frac{\bar{n}+1}{2\,\bar{n}+1}, \quad \beta \equiv \frac{\bar{n}}{2\,\bar{n}+1}, \quad (41)$$

and

$$\bar{s} \equiv e^{-\frac{1}{2}\tau(2\,\bar{n}+1)}, \quad \bar{p} = 1 - \bar{s}, \quad (42)$$

where $\bar{s}$ and $\bar{p}$ are dependent on the mean number of excitations $\bar{n}$ in the bath. In the zero-temperature limit, i.e., $\bar{n} = 0$ and $\bar{s} = s$, Eq. (39) reduces to the purely dissipative ADC, and its Kraus operators are represented as

$$\mathbf{K}_{\text{ADC}} = \{\sqrt{s}\,|0\rangle\langle 0| + |1\rangle\langle 1|, \sqrt{p}\,|1\rangle\langle 0|\}. \quad (43)$$

Similarly, in the Bloch representation, the GADC can be described as an affine map of which the transformation matrix $A$ and the translation vector $\boldsymbol{c}$ are given Table I, and the Bloch vector $\boldsymbol{\omega}$ is mapped as

$$\mathcal{E}_{\text{GADC}}(\boldsymbol{\omega}) = (\sqrt{\bar{s}}\,\omega_x, \sqrt{\bar{s}}\,\omega_y, \bar{s}\,\omega_z - \bar{p}\,(\alpha - \beta))^{\text{T}}. \quad (44)$$

When $\alpha = 1$ and $\beta = 0$, Eq. (44) reduce to the ADC case. This indicates that the GADC squeezes the Bloch sphere into an ellipsoid and shifts it toward the north pole. The radius in the $xy$ plane is reduced by a factor $\sqrt{s}$, while in the $z$ direction it is reduced by a factor $s$. In the asymptotic limit $\tau \to \infty$, i.e., $s = 0$, $p = 1$, the Bloch vector becomes $\mathcal{E}_{\text{GADC}}(\boldsymbol{\omega}) = (0, 0, -(\alpha - \beta))^{\text{T}}$, which also implies that, under the ADC ($\bar{n} = 0$), the qubit finally stay in the ground state. Meanwhile, the analytical results of the two QFIs under the GADC (the finite temperature) and the ADC (the zero-temperature) are derived in Table I.

When $\theta = \pi/2$, the dynamics of the QFI $\mathcal{F}$, under the ADC, in terms of $\theta$ and $\phi$ is the same, namely $\mathcal{F}_\theta = \mathcal{F}_\phi = s$. As shown in Figs. 1(e) and 1(f), under the GADC and ADC, the QFIs for the different parameters decrease monotonically with time. It is also shown that the QFIs for finite temperature decay more rapidly than those for zero temperature.

### B. Numerical calculation with the hierarchy equation

In this section, we focus on a simple dissipative model of a two-level system interacting with a zero-temperature bosonic reservoir to explicitly illustrate the behaviors of the two QFI quantities during time evolution [31,44]. Here, we exactly examine this model by adopting the hierarchy equation method. The total Hamiltonian of the system and bath without performing the RWA is

$$H = \frac{1}{2}\omega_0\sigma_z + \sum_k \omega_k b_k^\dagger b_k + \sigma_x B, \quad (45)$$

with $B = \sum_k g_k b_k + \text{H.c.}$ Here, the first term is the free Hamiltonian of the qubit with transition frequency $\omega_0$, the second term denotes the environment part with the creation (annihilation) operators $b_k^\dagger$ ($b_k$) of the bath model with frequency $\omega_k$, and the last term is the interaction Hamiltonian between the system and bath equipped with the coupling

constant $g_k$. In the zero-temperature limit, the spectral density is generally represented by a Lorentzian [44,45],

$$J(\omega) = \frac{1}{\pi}\frac{\lambda\gamma}{(\omega - \omega_0)^2 + \gamma^2}, \quad (46)$$

where $\lambda$ reflects the system-bath coupling strength and $\gamma$ is the spectral width of the coupling, which is related to the reservoir correlation time scale $\tau_B \sim \gamma^{-1}$.

As is well known, this typical dissipative model is solvable under the RWA, which is effective in the weak-coupling limit [44,52]. With the RWA, the analytical time-evolution function of the system can be equivalently described as an ADC by redefining the Kraus operators Eq. (43) as

$$\widetilde{\mathbf{K}}_{\text{ADC}} = \{h(t)|0\rangle\langle 0| + |1\rangle\langle 1|, \sqrt{(1 - h^2(t))}|1\rangle\langle 0|\}, \quad (47)$$

where $h(t)$ is a crucial characteristic function as

$$h(t) = e^{-\gamma t/2}\left[\cosh\left(\frac{dt}{2}\right) + \frac{\gamma}{d}\sinh\left(\frac{dt}{2}\right)\right], \quad (48)$$

with $d = \sqrt{\gamma^2 - 4\lambda}$. From Eq. (44), the affine-mapped Bloch vector reads under this dissipative environment

$$\widetilde{\mathcal{E}}_{\text{ADC}}(\boldsymbol{\omega}) = (h(t)\,\omega_x, h(t)\,\omega_y, 1 - h^2(t))^{\text{T}}. \quad (49)$$

As shown in Table I, then, one can easily recover the result of the dynamical QFI in terms of $\phi$ given in Ref. [31],

$$\mathcal{F}_\phi = h^2(t). \quad (50)$$

With the hierarchy equation method, the exact dynamic of the system is derived as the following equation in the interaction picture [52]:

$$\rho_S^{(I)}(t) = \mathcal{T}\exp\left\{-\int_0^t dt_2 \int_0^{t_2} dt_1 V(t_2)^\times[C^R(t_2 - t_1)\right.$$
$$\left. \times V(t_1)^\times + iC^I(t_2 - t_1)V(t_1)^\circ]\right\}\rho_{S(0)}, \quad (51)$$

where $\mathcal{T}$ is the chronological time-ordering operator and, to simplify the description, we introduce two superoperators $A^\times B \equiv [A, B]$ and $A^\circ B \equiv \{A, B\}$. Assume that the initial state is taken as $\rho(0) = \rho_S(0) \otimes \rho_B$ with $\rho_B$ being in the vacuum state $\otimes_k |0_k\rangle$. Also, $C^R(t_2 - t_1)$ and $C^I(t_2 - t_1)$, respectively, correspond to the real and imaginary part of the bath time-correlation function, which is defined as

$$C(t_2 - t_1) \equiv \langle B(t_2)B(t_1)\rangle_B = \text{Tr}[B(t_2)B(t_1)\rho_B], \quad (52)$$

where $B(t) = \sum_k g_k b_k e^{-i\omega_k t} + \text{H.c.}$ Then the time-correlation function Eq. (52) becomes the exponential form

$$C(t_2 - t_1) = \lambda\exp[-(\gamma + i\omega_0)|t_2 - t_1|]. \quad (53)$$

With Eqs. (51) and (53), we further obtain the set of hierarchical equations of the qubit as [52]

$$\frac{\partial}{\partial t}\varrho_{\vec{n}}(t) = -(iH_S^\times + \vec{n}\cdot\vec{v})\varrho_{\vec{n}}(t) - i\sum_{k=1}^2 V^\times\varrho_{\vec{n}+\vec{e}_k}(t)$$
$$- i\frac{\lambda}{2}\sum_{k=1}^2 n_k[V^\times + (-1)^k V^\circ]\varrho_{\vec{n}-\vec{e}_k}(t), \quad (54)$$

where the subscript $\vec{n} = (n_1, n_2)$ is a two-dimensional index with $n_{1(2)} \geqslant 0$, and $\rho_S(t) \equiv \varrho_{(0,0)}(t)$. The vectors are
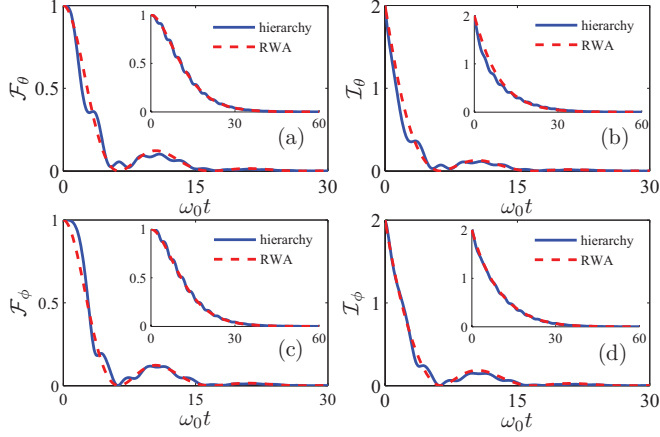
FIG. 2. (Color online) Two QFIs, Eq. (2) (a),(b) and Eq. (16) (c),(d), vs time for different parameters initially embedded in the qubit under the dissipative process. The solid lines display the numerical results by using the hierarchy equation method. These are compared to the analytical results with RWA (dashed lines), all plotted in the non-Markovian regime ($\lambda = 0.1\gamma$). The insets show the Markovian regime ($\lambda = 0.01\gamma$)

$\vec{e}_1 = (1, 0)$, $\vec{e}_2 = (0, 1)$, and $\vec{v} = (v_1, v_2) = (\gamma - i\omega_0, \gamma + i\omega_0)$. We emphasize that $\varrho_{\vec{n}}(t)$, with $\vec{n} \neq (0, 0)$, are auxiliary operators introduced only for the sake of computing; they are not density matrices, and are all set to be zero at $t = 0$. Through solving the above hierarchy equations, the dynamics of the system can be exactly determined without making the RWA.

Figure 2 displays the dynamics of the QFI of Eq. (2) and the variant QFI of Eq. (16) versus time for different parameters initially encoded in the qubit state. The spectral width of the coupling is set by $\gamma = 0.2\omega_0$. In the Markovian regime (inset plots with $\lambda = 0.01\gamma$), the QFIs $\mathcal{F}_{\theta(\phi)}$ and $\mathcal{I}_{\theta(\phi)}$ monotonically go to zero. Both the numerical and the analytical results are consistent in the weak-coupling limit, while in the non-Makovian regime ($\gamma = 0.1\lambda$), due to the strong coupling with the reservoir, the dynamics of these two information quantities exhibits the oscillations and revivals over time. The times when $\mathcal{I}_{\theta(\phi)}$ vanishes completely coincide with those for $\mathcal{F}_{\theta(\phi)}$. The surprising aspect here is that the quantities of $\mathcal{I}_{\theta(\phi)}$ for the two parameters $\theta$ and $\phi$ decrease quickly to zero from the initial value of 2, and then later on revive with almost the same amount as $\mathcal{F}_{\theta(\phi)}$. Since the hierarchical equations we obtained exactly depict the dynamics of the system, the oscillating deviations between the numerical and the analytical results can be interpreted as the contribution of the counter-rotating-wave terms which have been omitted by making the RWA [52]. Such deviations behave evidently for both information quantities in terms of $\theta$. As shown in Ref. [31], they addressed these oscillations and revivals in Figs. 2(a) and 2(b) by introducing the definition of the QFI flow. Analogously, we also introduce a variant QFI flow (or skew information flow) as the change rate of information quantity $\mathcal{I}$, i.e., $\sigma := \partial \mathcal{I}_\lambda / \partial t$. Also, $\sigma > 0$ indicates that there is an information flow from the environment to the system, corresponding to the revivals, and $\sigma < 0$ denotes the flow from the system to the environment, accounting for the decays, as shown in Figs. 2(c) and 2(d).

## IV. GENERALIZATION

### A. Representation of the QFI in terms of the generalized Bloch vector for a qudit system

We have examined the QFIs under decoherence for a single qubit in the Bloch representation. Now, we consider a more general case, i.e., the qudit (a $d$-dimensional quantum system). A general qudit state can be written in the Bloch representation as [62,63]

$$\rho = \frac{1}{d}\mathbb{1}_d + \frac{1}{2}\boldsymbol{\omega} \cdot \hat{\boldsymbol{\eta}}, \tag{55}$$

where $\mathbb{1}_d$ is a $d \times d$ identity operator, $\hat{\boldsymbol{\eta}} = \{\hat{\eta}_i\}_{i=1}^{d^2-1}$ are the generators of the Lie algebra su$(d)$ (see Appendix A), and $\boldsymbol{\omega} \in \mathbb{R}^{d^2-1}$ denotes the generalized Bloch vector whose $i$th element is Tr$(\rho\,\hat{\eta}_i)$.

We have the relation

$$1/d \leqslant \text{Tr}(\rho^2) \leqslant 1, \tag{56}$$

where Tr$(\rho^2)$ is the purity, which is equal to 1 corresponding to pure states and $1/d$ corresponding to mixed states. With Eq. (55), we get

$$\text{Tr}(\rho^2) = \frac{1}{d} + \frac{1}{2}|\boldsymbol{\omega}|^2 \tag{57}$$

by using the following relation:

$$\text{Tr}[(\boldsymbol{a} \cdot \hat{\boldsymbol{\eta}})(\boldsymbol{b} \cdot \hat{\boldsymbol{\eta}})] = 2\,\boldsymbol{a} \cdot \boldsymbol{b}. \tag{58}$$

Thus, from Eqs. (56) and (57), we obtain the length of the generalized Bloch vector satisfying

$$0 \leqslant \omega \leqslant \sqrt{2(d-1)/d}, \tag{59}$$

where the first equality holds for the maximal mixed state and the second for pure states.

Due to the completeness of the generators of Lie algebra, any Hermitian matrix can be described by the common set of generators. Based on this representation, we give the expressions of the two QFIs in terms of the Bloch vector. First, we consider the QFI in Eq. (2). $\mathcal{F}_\lambda$ can be represented as

$$\mathcal{F}_\lambda = \begin{cases} (\partial_\lambda \boldsymbol{\omega})^{\text{T}} \mathcal{M}^{-1} \partial_\lambda \boldsymbol{\omega}, & \omega < \sqrt{2(d-1)/d}, \\ |\partial_\lambda \boldsymbol{\omega}|^2, & \omega = \sqrt{2(d-1)/d}, \end{cases} \tag{60}$$

where $\mathcal{M}$ is a real symmetry matrix defined as

$$\mathcal{M} = \frac{2}{d}\mathbb{1}_{d^2-1} - \boldsymbol{\omega}\boldsymbol{\omega}^{\text{T}} + G. \tag{61}$$

The superscript T in the above equations denotes the transpose operation and $\mathcal{M}^{-1}$ denotes the matrix inverse of $\mathcal{M}$. $\mathbb{1}_{d^2-1}$ is the identity matrix of dimension $d^2 - 1$ and $G$ is a $(d^2 - 1) \times (d^2 - 1)$ real symmetric matrix whose $ij$ element is

$$[G]_{ij} = \sum_{k=1}^{d^2-1} g_{ijk}\,\omega_k, \tag{62}$$

where $g_{ijk}$ is the completely symmetric tensor defined in Eq. (A7). Hence, $\mathcal{M}$ is also real symmetric matrix. Since $\mathcal{M}$ may have some zero eigenvalues, the inverse is defined on the support of $\mathcal{M}$ [61]. Here, the first line of Eq. (60) only applies to mixed states, and the detailed derivation can be found in Appendix B.

For pure states, $\mathcal{F}_\lambda$ is generally expressed as the norm of the derivative of the Bloch vector shown in Eq. (60). It can be easily derived using Eq. (58) and following the same procedure used in deriving the second line of Eq. (11).

From Eq. (61), we can see that the matrix $\mathcal{M}$ is dependent on $\boldsymbol{\omega}$. Then we can conclude that $\mathcal{F}_\lambda$ given by Eq. (60) only depends on two elements: the Bloch vector of the density matrix and its derivative. Moreover, it should be emphasized that Eq. (60) is also valid for an arbitrary quantum state, since a density matrix can always be expressed as the form of Eq. (55) by expanding over the generators of the Lie algebra.

When $d = 2$, we have $G = 0$, due to $g_{ijk} = 0$. Then, the real symmetric matrix $\mathcal{M}$ reduces to

$$\mathcal{M} = \mathbb{1}_3 - \boldsymbol{\omega}\boldsymbol{\omega}^{\mathrm{T}}. \tag{63}$$

The inverse of $\mathcal{M}$ is verified as

$$\mathcal{M}^{-1} = \mathbb{1}_3 + \frac{\boldsymbol{\omega}\,\boldsymbol{\omega}^{\mathrm{T}}}{1 - |\boldsymbol{\omega}|^2}. \tag{64}$$

Substituting the above equation into Eq. (60) finally recovers the first line of Eq. (11).

We next take account of the QFI in Eq. (16). We first expand

$$\sqrt{\rho} = y\mathbb{1}_d + \boldsymbol{x} \cdot \hat{\boldsymbol{\eta}}. \tag{65}$$

Then $\mathcal{I}_\lambda$ can be represented as follows:

$$\mathcal{I}_\lambda = \begin{cases} 8\left[(\partial_\lambda y)^2 + \frac{2}{d}|\partial_\lambda \boldsymbol{x}|^2\right], & \omega < \sqrt{2(d-1)/d}, \\ 2|\partial_\lambda \boldsymbol{\omega}|^2, & \omega = \sqrt{2\,(d-1)\,/d}, \end{cases} \tag{66}$$

where $y$ and $\boldsymbol{x}$ are completely determined by the following $d^2$ quadratic nonlinear equations:

$$y^2 + \frac{2}{d}|\boldsymbol{x}|^2 = \frac{1}{d}, \tag{67}$$

$$2yx_k + \sum_{i,j=1}^{d^2-1} g_{ijk}x_i x_j = \frac{\omega_k}{2} \tag{68}$$

for $k = 1, 2, \ldots, d^2 - 1$. The first line of the above equation is applicable for mixed states, and the detailed derivation is given in Appendix C.

For pure states, $\mathcal{I}_\lambda$ is generally expressed as the norm of the derivative of the Bloch vector up to a factor of 2 shown in Eq. (66). It can be obtained by using Eq. (58) and following the same procedure used in deriving the second line of Eq. (25).

For the case of $d = 2$, Eqs. (67) and (68) reduce to

$$y^2 + |\boldsymbol{x}|^2 = \tfrac{1}{2}, \tag{69}$$

$$4y\boldsymbol{x} = \boldsymbol{\omega}, \tag{70}$$

with $g_{ijk} = 0$. By solving the above equations (see Appendix C), one can obtain

$$y = \frac{\sqrt{1 + \sqrt{1 - |\boldsymbol{\omega}|^2}}}{2}, \tag{71}$$

$$\boldsymbol{x} = \frac{\boldsymbol{\omega}}{2\sqrt{1 + \sqrt{1 - |\boldsymbol{\omega}|^2}}}. \tag{72}$$

Inserting the above solutions into the first line of Eq. (66) and making some simplification recovers the first line given in Eq. (25).

## B. QFI for an $N$-qubit system in a noisy environment

Below, we study the dynamic of the QFI for an $N$-qubit system in a noisy environment. In the Bloch representation, the two QFIs for the qudit are described in terms of the generalized Bloch vector $\boldsymbol{\omega}$, as is shown in Eqs. (60) and (66), respectively. The Bloch vector is assumed to be the function of an unknown parameter $\lambda$ on the system. Meanwhile, we emphasize that Eqs. (60) and (66) are also applicable for the multi-qubit system with exchange symmetry. A collection of $N$ qubits is represented by the collective operators [64]

$$J_\alpha = \sum_{i=1}^{N} \frac{\sigma_{i\alpha}}{2} \ (\alpha = x, y, z), \tag{73}$$

where $\sigma_{i\alpha}$ denotes the Pauli matrix of the $i$th qubit. Such an $N$-qubit ensemble with total angular momentum $j = N/2$ can be approximately viewed as a qudit system when it has the symmetry under the exchange of two qubits. The collective basis of this system is $\{|j,m\rangle\}$ for $m = 0, \pm 1, \pm 2, \ldots, \pm j$, which is the so-called Dicke state, $J_z|j,m\rangle = m|j,m\rangle$. Hence, Eqs. (60) and (66) are also valid for those multi-qubit systems.

Assume that the dimension of the decohered state $\mathcal{E}(\rho)$ is the same as that of $\rho$. Similar to Eq. (30), an $N$-qubit system with exchange symmetry described by Eq. (55) under decoherence can be expressed as [40,61]

$$\mathcal{E}(\rho) = \frac{1}{d}\mathbb{1}_d + \frac{1}{2}(A\,\boldsymbol{\omega} + \boldsymbol{c}) \cdot \hat{\boldsymbol{\eta}}, \tag{74}$$

with $d = N + 1$. Here, $A$ is a matrix of dimension $d^2 - 1$ with elements

$$A_{ij} = \tfrac{1}{2}\mathrm{Tr}\,[\hat{\eta}_i\,\mathcal{E}(\hat{\eta}_j)], \tag{75}$$

and $\boldsymbol{c}$ is a $(d^2 - 1)$-dimensional vector with elements

$$c_i = \frac{1}{d}\mathrm{Tr}\,[\hat{\eta}_i\,\mathcal{E}(\mathbb{1}_d)]. \tag{76}$$

Equation (74) illustrates that a Markovian quantum dynamic can be geometrically described as an affine transformation, i.e.,

$$\mathcal{E} : \ \boldsymbol{\omega} \mapsto A\,\boldsymbol{\omega} + \boldsymbol{c}. \tag{77}$$

As we mentioned at the beginning of Sec. III, in the parameter estimation, the unknown parameter is generally imprinted into the probes through unitary or nonunitary evolution [15]. It is noted that Eq. (60) is applicable to the cases with different parametrization processes by replacing the Bloch vector $\boldsymbol{\omega}$ with the affine-mapped Bloch vector $\mathcal{E}(\boldsymbol{\omega})$.

To be more specific, we consider an experimentally realizable Ramsey interferometry [65] to estimate a physical parameter in a Bose-Einstein condensate (BEC) of $N$ two-level atoms interacting with a common thermal reservoir. This experiment we model is shown schematically in Fig. 3. Those two-level atoms may be considered as qubits or probes, which are prepared in an $N$-qubit Greenberger-Horne-Zeilinger
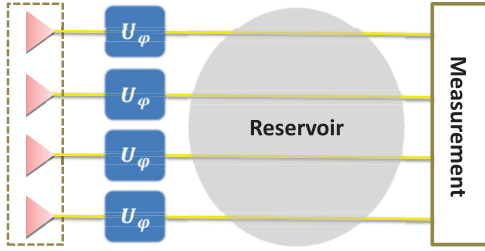
FIG. 3. (Color online) The schematic representation of Ramsey interferometry in the presence of collisional dephasing.

(GHZ) state (or Schrödinger-cat state),

$$|\psi_{\text{GHZ}}\rangle = \frac{1}{\sqrt{2}}(|0\rangle^{\otimes N} + |1\rangle^{\otimes N}). \tag{78}$$

If all the qubits are initially prepared in $|0\rangle$, then a GHZ state is generated by putting a Hadamard gate on the first qubit, followed by a sequence of controlled-NOT gates linking the first one with each of the remaining ones [11,13,65]. It is well known that such a state saturates the ultimate Heisenberg limit (HL) $1/N$ on precision of measurement. This result gives a quadratic improvement over the standard quantum limit (SQL), which is achievable with product states [11,65].

As is shown in Fig. 3, the parameter $\varphi$ of interest is unitarily imprinted on the state of the probe qubits. The unitary operator is given by

$$U_{\varphi}^{\text{tot}} = U_{\varphi}^{\otimes N} = \left[\exp\left(-i\frac{\varphi}{2}\sigma_z\right)\right]^{\otimes N} = e^{-i\varphi J_z}, \tag{79}$$

where $J_z$ is the $z$ component of the total angular momentum for all qubits [65]. After the unitary evolution, the state of the probes becomes

$$|\tilde{\psi}_{\text{GHZ}}\rangle = \frac{1}{\sqrt{2}}(|0\rangle^{\otimes N} + e^{i N\varphi}|1\rangle^{\otimes N})$$
$$= \frac{1}{\sqrt{2}}\left(\left|\frac{N}{2},\frac{N}{2}\right\rangle + e^{i N\varphi}\left|\frac{N}{2},-\frac{N}{2}\right\rangle\right), \tag{80}$$

up to a global phase factor $e^{-iN\varphi/2}$. The second equality above is valid in the standard representation of the generator $J_z$. According to Appendix D, the Bloch vector of the state of

Eq. (80) reads

$$\boldsymbol{\omega}_{\varphi} = \left(\underbrace{\cos(N\varphi),0,\ldots,0}_{(d^2-d)/2}, \underbrace{\sin(N\varphi),0,\ldots,0}_{(d^2-d)/2},\right.$$
$$\left.\frac{1}{2},\ldots,\frac{1}{\sqrt{2m(m+1)}},\ldots,\frac{1}{\sqrt{2(d-1)(d-2)}},\right.$$
$$\left.\frac{2-d}{\sqrt{2d(d-1)}}\right)^{\text{T}} \tag{81}$$

for $m = 1,\ldots,d-2$. For the sake of clarity, we take $N = 2$ (i.e., $d = 3$) for example. The Bloch vector for $N = 2$ in Eq. (81) becomes

$$\boldsymbol{\omega}_{\varphi} = \left(\cos(2\varphi),0,0,\sin(2\varphi),0,0,\frac{1}{2},-\frac{1}{2\sqrt{3}}\right)^{\text{T}}$$

of dimension 8. As is shown in Eq. (81), $\boldsymbol{\omega}_{\varphi}$ only contains two $\varphi$-dependent elements. From Eq. (60), we find that those $\varphi$-independent elements of $\boldsymbol{\omega}_{\varphi}$ will not contribute to the computation of $\mathcal{F}_{\varphi}$.

In the realistic experiment, decoherence always exists. As is shown in Fig. 3, we consider the effect of the collisional dephasing on this measurement protocol, which is induced by the interaction between the qubits and the common thermal reservoir [66,67]. The master equation of the system in the Lindblad form can be described as [67,68]

$$\dot{\rho}(t) = \mathcal{L}\rho \equiv \gamma\left[2\hat{J}_z\rho(t)\hat{J}_z - \rho(t)\hat{J}_z^2 - \hat{J}_z^2\rho(t)\right], \tag{82}$$

where $\mathcal{L}$ denotes the Lindblad superoperator, $\gamma$ denotes the dephasing rate, and $\rho$ is the reduced density operator of the system in the interaction picture. For the single-qubit case, Eq. (82) reduces to

$$\dot{\rho}(t) = \mathcal{L}\rho \equiv \frac{\gamma}{2}\left[\sigma_z\rho(t)\sigma_z - \rho(t)\right], \tag{83}$$

which corresponds to a single-qubit dephasing channel (i.e., DPC). Here, we use the interaction representation, which does not affect the result of the calculation, since the QFI $\mathcal{F}$ remains invariant under the unitary evolution being independent of the parameter $\varphi$. From Eq. (82), the time evolution of the density matrix elements is given as follows:

$$\rho_{m,n}(t) = \langle j,m|\rho(t)|j,n\rangle = \rho_{m,n}(0)e^{-(m-n)^2\tau}, \tag{84}$$

where we have set $\tau = \gamma t$. In the Bloch representation, the corresponding affine transformation matrix for the collisional dephasing in Eq. (82) can be obtained as
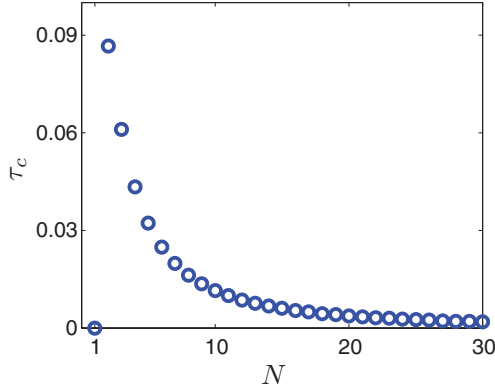
$$A = \text{diag}\left(\underbrace{e^{-N^2\tau},e^{-(N-1)^2\tau},e^{-(N-1)^2\tau},e^{-(N-2)^2\tau},\ldots,e^{-4\tau},\overbrace{e^{-\tau},\ldots,e^{-\tau}}^{d-1}}_{(d^2-d)/2}\right.$$

$$\left.\times\underbrace{e^{-N^2\tau},e^{-(N-1)^2\tau},e^{-(N-1)^2\tau},e^{-(N-2)^2\tau},\ldots,e^{-4\tau},\overbrace{e^{-\tau},\ldots,e^{-\tau}}^{d-1}}_{(d^2-d)/2},\underbrace{1,1,\ldots,1}_{d-1}\right) \tag{85}$$

and $\boldsymbol{c} = \boldsymbol{0}$ (see Appendix D). Apparently, both the transformation matrix $A$ and the translation vector $\boldsymbol{c}$ are independent of $\varphi$. After the dephasing process, the Bloch vector of Eq. (81) is affine-mapped as

$$\mathcal{E}(\boldsymbol{\omega}_{\varphi}) = \left(e^{-N^2\tau}\cos(N\varphi),0,\ldots,0,e^{-N^2\tau}\sin(N\varphi),0,\ldots,0,\frac{1}{2},\ldots,\frac{1}{\sqrt{2k(k+1)}},\ldots,\frac{1}{\sqrt{2(d-1)(d-2)}},\frac{2-d}{\sqrt{2d(d-1)}}\right)^{\text{T}}, \tag{86}$$

FIG. 4. (Color online) Plot of the characteristic time $\tau_c$ in Eq. (88) (blue dash-circle curve).

which is given by inserting $A$ of Eq. (85) and $c = 0$ into Eq. (77). The dynamics of the QFI associated to the parameter $\varphi$ may be evaluated as, from Eqs. (60) and (86),

$$\mathcal{F}_\varphi = N^2 e^{-2N^2\tau}, \tag{87}$$

which shows that the quantity of the QFI is monotonically decreased by a factor of $e^{-2N^2\tau}$. This result is consistent with Ref. [69], while the dynamics of the QFI under the local dephasing process was studied in Refs. [6,7].

To clearly see the effect of the decoherence process, we define a time scale $\tau_c$ which is the time over which the QFI reduces from the HL (i.e., $\mathcal{F}_\varphi = N^2$) to the SQL (i.e., $\mathcal{F}_\varphi = N$) [6]. For the collisional dephasing, the characteristic time reads

$$\tau_c = \frac{\log N}{2N^2}. \tag{88}$$

After $\tau_c$ above, the GHZ state cannot be used to perform over shot-noise estimation. As is plotted in Fig. 4, the characteristic time decreases exponentially as $N$ increases. This illustrates that the advantage of a GHZ state deteriorates in the case of collisional dephasing.

We further observe the optimal precision of frequency measurements in this situation. In the standard Ramsey spectroscopy, the parameter of interest is the frequency of the atomic transition which is denoted as $\omega'$, and the uncertainty of the frequency depends on the available physical resources, which we take to be the probe size $N$ and the total time $T$ of the experiment. Taking the time of a single shot as $t$, the number of trials is $\nu = T/t$, and the quantum Cramér-Rao inequality of Eq. (6) can be rewritten as

$$\Delta\omega'\sqrt{T} \geqslant \frac{1}{\sqrt{\mathcal{F}_{\omega'}/t}} \tag{89}$$

in the asymptotic limit $\nu \to \infty$ [14]. As is well known, entangled states may provide a HL-scaling limit on the measurement precision in the absence of noise. In the seminal paper of Refs. [13,14], it was found that GHZ states do not offer any improvement in precision in the presence of the local dephasing, and they only provide a SQL-scaling limit (i.e., $\Delta\omega'\sqrt{T} \sim 1/\sqrt{N}$). In addition, an achievable lower bound for the ultimate limit of precision in noisy systems is investigated in Refs. [15,16]. It is shown that when local decoherence is taken into account, the maximal possible

quantum enhancement amounts generically to a constant factor in the asymptotic limit of infinite probes.

Now, we consider the effect of collective dephasing on the precision measurement. From Eq. (87), we can directly obtain the QFI in terms of $\omega'$ as

$$\mathcal{F}_{\omega'} = N^2 e^{-2N^2\tau} t^2 \tag{90}$$

by setting $\varphi = \omega't$. Taking the optimal time as $t_{\text{opt}} = 1/(2\gamma N^2)$ as is shown in Refs. [13,14], the ultimate precision of frequency reads

$$\Delta\omega'\sqrt{T} \geqslant \sqrt{2\gamma e} \tag{91}$$

by substituting Eq. (90) into Eq. (89). Counterintuitively, this result shows that GHZ states cannot even provide a SQL scaling of precision in the presence of the collective dephasing. This indicates that the collective noise may do serious damage to the quantum parameter estimation.

## V. DISCUSSION AND CONCLUSION

We have discussed the time evolution of the two variant versions of the QFIs in the presence of quantum noises. With the help of the Bloch representation, we derived the explicit formula of the two information quantities for a single-qubit system. The analytical expressions of the dynamics of the two QFIs under three typical quantum decoherence channels were obtained. Both information quantities in those channels are decreased monotonically with time except for the case in which the $\mathcal{F}_\theta$ remained invariant under PDC. It manifested that the QFI defined in Eq. (2) about the amplitude parameter $\theta$ is robust for the PDC.

We also considered a simple dissipative model of a single-qubit coupling with a bosonic reservoir at zero temperature. By applying the hierarchy equation method, we exactly calculated the dynamical QFIs during time evolution. We found that the numerical results qualitatively coincided with the analytical ones using the RWA. The deviation between them can be attributed to the contribution of the counter-rotating-wave terms. In the weak-coupling regime, we observed that two QFIs about different parameters were monotonically decreased. When the strength of the coupling became more stronger, the behavior of the non-Markovian could be observed from the QFIs perspective.

Finally, we generalized the results to the qudit system, expressing the two QFIs in terms of the generalized Bloch vector. Those expressions were valid for the $N$-qubit system with symmetry exchange. We also considered the QFI in the presence of the collisional dephasing with the initial state being prepared as a GHZ state. The affine matrices for this dephasing process were derived, and the Bloch vector of the GHZ state was also expressed as the Bloch vector. We found that the dynamical QFI decreases exponentially by a factor of $e^{-2N^2\tau}$.

## APPENDIX A: GENERATORS OF THE LIE ALGEBRA su($d$)

In group theory, the generators of the Lie algebra have the following properties: (i) Hermitian,

$$\hat{\eta}_i^\dagger = \hat{\eta}_i; \tag{A1}$$

(ii) traceless,

$$\mathrm{Tr}\,\hat{\eta}_i = 0; \tag{A2}$$

(iii) orthogonality and normalization with respect to the trace metric relation,

$$\tfrac{1}{2}\mathrm{Tr}(\hat{\eta}_i\,\hat{\eta}_j) = \delta_{ij}. \tag{A3}$$

Moreover, they also satisfy two relations as follows, characterized by the structure constants $f_{ijk}$ and $g_{ijk}$:

$$[\hat{\eta}_i, \hat{\eta}_j] = 2\,i \sum_k f_{ijk}\,\hat{\eta}_k, \tag{A4}$$

$$\{\hat{\eta}_i, \hat{\eta}_j\} = \frac{4}{d}\,\delta_{ij}\,\mathbb{1}_d + 2\sum_k g_{ijk}\,\hat{\eta}_k, \tag{A5}$$

where $\mathbb{1}_d$ is the unit matrix of dimension $d$, and $f_{ijk}$ ($g_{ijk}$) denotes the completely antisymmetric (symmetric) tensor. The structure constants are determined by

$$f_{ijk} = \frac{1}{4\,i}\,\mathrm{Tr}\,([\hat{\eta}_i, \hat{\eta}_j]\hat{\eta}_k), \tag{A6}$$

$$g_{ijk} = \frac{1}{4}\,\mathrm{Tr}\,(\{\hat{\eta}_i, \hat{\eta}_j\}\hat{\eta}_k). \tag{A7}$$

Employing the completeness relation of the generators of su($d$), one can expand an arbitrary $d$-dimensional Hermitian matrix $X$ as

$$X = \frac{1}{d}\,\mathrm{Tr}\,(X)\,\mathbb{1}_d + \sum_{k=1}^{d^2-1} x_k\,\hat{\eta}_k, \quad x_k \in \mathbb{R}, \tag{A8}$$

with $x_k = \mathrm{Tr}\,(X\,\hat{\eta}_k)$.

Below, we systematically construct the generators $\hat{\eta} = \{\eta_j\}_{j=1}^{d^2-1}$ of the Lie algebra su($d$) which are given as follows [62,63]. On a $d$-dimensional Hilbert space $\mathcal{H} \in \mathbb{C}^d$ spanned by an orthonormal set of states $\{|\,m\,\rangle\}_{m=1}^d$, we first construct two sets of block off-diagonal Hermitian traceless matrices,

$$\hat{\mathcal{S}}_{m,n} = |m\rangle\langle n| + |n\rangle\langle m|, \tag{A9}$$

$$\hat{\mathcal{A}}_{m,n} = -i\,(|m\rangle\langle n| - |n\rangle\langle m|) \tag{A10}$$

for $1 \leqslant m < n \leqslant d$. The above two sets contain the same number of elements as $(d^2 - d)/2$. Then, we construct $d - 1$ real diagonal traceless matrices

$$\hat{\mathcal{D}}_k = \sqrt{\frac{2}{k(k+1)}}\left[\sum_{m=1}^k |m\rangle\langle m| - k\,|k+1\rangle\langle k+1|\right] \tag{A11}$$

for ($1 \leqslant k \leqslant d - 1$). Hitherto, the generators for the Lie algebra su($d$) are obtained by the new set [62,63],

$$\{\hat{\eta}_i\}_{i=1}^{d^2-1} = \{\hat{\mathcal{S}}_{m,n}, \hat{\mathcal{A}}_{m,n}, \hat{\mathcal{D}}_k\}. \tag{A12}$$

The generators for $d = 2$ coincide with the Pauli matrices with the structure constants $f_{ijk}$ being the Levi-Civita symbol $\epsilon_{ijk}$ and $g_{ijk} = 0$. The generators of su(3) are described by the Gell-Mann matrices given by [63]

$$
\hat{\eta}_1 = \begin{pmatrix} 0 & 0 & 1 \\ 0 & 0 & 0 \\ 1 & 0 & 0 \end{pmatrix}, \qquad
\hat{\eta}_2 = \begin{pmatrix} 0 & 1 & 0 \\ 1 & 0 & 0 \\ 0 & 0 & 0 \end{pmatrix},
$$
$$
\hat{\eta}_3 = \begin{pmatrix} 0 & 0 & 0 \\ 0 & 0 & 1 \\ 0 & 1 & 0 \end{pmatrix}, \qquad
\hat{\eta}_4 = \begin{pmatrix} 0 & 0 & -i \\ 0 & 0 & 0 \\ i & 0 & 0 \end{pmatrix},
$$
$$
\hat{\eta}_5 = \begin{pmatrix} 0 & -i & 0 \\ i & 0 & 0 \\ 0 & 0 & 0 \end{pmatrix}, \qquad
\hat{\eta}_6 = \begin{pmatrix} 0 & 0 & 0 \\ 0 & 0 & -i \\ 0 & i & 0 \end{pmatrix},
$$
$$
\hat{\eta}_7 = \begin{pmatrix} 1 & 0 & 0 \\ 0 & -1 & 0 \\ 0 & 0 & 0 \end{pmatrix}, \qquad
\hat{\eta}_8 = \frac{1}{\sqrt{3}}\begin{pmatrix} 1 & 0 & 0 \\ 0 & 1 & 0 \\ 0 & 0 & -2 \end{pmatrix}. \tag{A13}
$$

## APPENDIX B: DERIVATION OF EQ. (60)

Now, we provide the detailed derivation of the first line of Eq. (60). To express $\mathcal{F}_\lambda$ in terms of the Bloch vector, we should first write all the Hermitian operator in the same representation, expanding them over the common generators of the Lie algebra su($d$) [61]. The density matrix $\rho$ is described by Eq. (55), and the SLD operator is supposed to be expanded as

$$L = a\mathbb{1}_d + \boldsymbol{b} \cdot \hat{\boldsymbol{\eta}}, \tag{B1}$$

where $a$ and $\boldsymbol{b}$ are, respectively, a real number and a real vector to be determined.

Suppose $\rho$ contains some unknown parameter $\lambda$, i.e., the Bloch vector $\boldsymbol{\omega}$ is $\lambda$-dependent. Then we have

$$\partial_\lambda \rho = \tfrac{1}{2}\,(\partial_\lambda \boldsymbol{\omega})^{\mathrm{T}}\,\hat{\boldsymbol{\eta}}. \tag{B2}$$

By substituting Eqs. (B1) and (B2) into Eq. (2), we find that $\mathcal{F}_\lambda$ can be rewritten as

$$\mathcal{F}_\lambda = (\partial_\lambda \boldsymbol{\omega})^{\mathrm{T}}\,\boldsymbol{b}. \tag{B3}$$

Here, we use Eq. (58) and the traceless property of generators. Equation (B3) shows that when $\boldsymbol{b}$ is derived, then the problem is solved.

To determine $\boldsymbol{b}$, we should use Eq. (3). Furthermore, by using Eq. (A5), we have the following relation:

$$
\{\boldsymbol{a} \cdot \hat{\boldsymbol{\eta}}, \boldsymbol{b} \cdot \hat{\boldsymbol{\eta}}\} = \sum_{ij} a_i b_j \{\hat{\eta}_i, \hat{\eta}_j\}
$$
$$
= \frac{4}{d}\,\boldsymbol{a}^{\mathrm{T}}\boldsymbol{b}\,\mathbb{1}_d + 2\sum_{ijk} g_{ijk} a_i b_j\,\hat{\eta}_k. \tag{B4}
$$

With the help of Eqs. (55), (B1), and (B4), the right-hand side (RHS) of Eq. (3) reads

$$
\begin{aligned}
\frac{1}{2}\{\rho, L\} &= \frac{1}{2}\left( \left\{ \frac{\mathbb{1}}{d}, a\mathbb{1} + \boldsymbol{b}\cdot\hat{\boldsymbol{\eta}} \right\} \right. \\
&\quad + \left\{ \frac{1}{2}\boldsymbol{\omega}\cdot\hat{\boldsymbol{\eta}}, a\mathbb{1} \right\} + \left. \left\{ \frac{1}{2}\boldsymbol{\omega}\cdot\hat{\boldsymbol{\eta}}, \boldsymbol{b}\cdot\hat{\boldsymbol{\eta}} \right\} \right) \\
&= \frac{1}{d}(a + \boldsymbol{\omega}^{\mathrm{T}}\boldsymbol{b})\mathbb{1} \\
&\quad + \sum_k \left( \frac{1}{d}b_k + \frac{1}{2}a\omega_k + \frac{1}{2}\sum_{ij} g_{ijk}\omega_i b_j \right)\eta_k.
\end{aligned}
$$

The left-hand side (LHS) of Eq. (3) is given by Eq. (B2). By comparing the terms on both sides of Eq. (3), one obtains

$$
a + \boldsymbol{\omega}^{\mathrm{T}}\boldsymbol{b} = 0, \tag{B5}
$$

$$
\begin{aligned}
(\partial_\lambda\boldsymbol{\omega})^{\mathrm{T}}\hat{\boldsymbol{\eta}} &= \sum_k \left( \frac{2}{d}b_k + a\omega_k + \sum_{ij} g_{ijk}\omega_i b_j \right)\eta_k \\
&= \frac{2}{d}\boldsymbol{b}^{\mathrm{T}}\hat{\boldsymbol{\eta}} + a\boldsymbol{\omega}^{\mathrm{T}}\hat{\boldsymbol{\eta}} + \sum_{ijk} g_{ijk}\omega_i b_j\hat{\eta}_k \\
&= \frac{2}{d}\boldsymbol{b}^{\mathrm{T}}\hat{\boldsymbol{\eta}} + a\boldsymbol{\omega}^{\mathrm{T}}\hat{\boldsymbol{\eta}} + \sum_{jk} b_j G_{jk}\hat{\eta}_k \\
&= \frac{2}{d}\boldsymbol{b}^{\mathrm{T}}\hat{\boldsymbol{\eta}} + a\boldsymbol{\omega}^{\mathrm{T}}\hat{\boldsymbol{\eta}} + \boldsymbol{b}^{\mathrm{T}}G\hat{\boldsymbol{\eta}}. \tag{B6}
\end{aligned}
$$

Here, the matrix element of $G$ in Eq. (B6) is given by $G_{jk} = \sum_i g_{ijk}\omega_i$ satisfying $G_{jk} = G_{kj}$. With Eq. (B5), we have

$$
a = -\boldsymbol{\omega}^{\mathrm{T}}\boldsymbol{b} = -\boldsymbol{b}^{\mathrm{T}}\boldsymbol{\omega}. \tag{B7}
$$

By insetting the above equation into Eq. (B6), we obtain

$$
(\partial_\lambda\boldsymbol{\omega})^{\mathrm{T}}\hat{\boldsymbol{\eta}} = \boldsymbol{b}^{\mathrm{T}}\left( \frac{2}{d} - \boldsymbol{\omega}\boldsymbol{\omega}^{\mathrm{T}} + G \right)\hat{\boldsymbol{\eta}}, = \boldsymbol{b}^{\mathrm{T}}\mathcal{M}\hat{\boldsymbol{\eta}}, \tag{B8}
$$

by setting

$$
\mathcal{M} \equiv \frac{2}{d} - \boldsymbol{\omega}\boldsymbol{\omega}^{\mathrm{T}} + G.
$$

Hence, Eq. (B8) directly gives the following equation:

$$
(\partial_\lambda\boldsymbol{\omega})^{\mathrm{T}} = \boldsymbol{b}^{\mathrm{T}}\mathcal{M}. \tag{B9}
$$

Suppose that we have the inverse matrix $\mathcal{M}^{-1}$. After Eq. (B11), we will make further discussions about $\mathcal{M}^{-1}$. We have

$$
\boldsymbol{b} = \mathcal{M}^{-1}(\partial_\lambda\boldsymbol{\omega}) \tag{B10}
$$

from Eq. (B9). Finally, inserting Eq. (B10) into Eq. (B3) yields

$$
\mathcal{F}_\lambda = (\partial_\lambda\boldsymbol{\omega})^{\mathrm{T}}\mathcal{M}^{-1}(\partial_\lambda\boldsymbol{\omega}). \tag{B11}
$$

To calculate $\mathcal{F}_\lambda$, we need to find the inverse of $\mathcal{M}$. Generally, it may or may not exist, i.e., $\mathcal{M}$ may have some zero eigenvalues. In this case, we define $\mathcal{M}^{-1}$ on the support of $\mathcal{M}$, i.e., suppl($\mathcal{M}$), which is defined as a space spanned by those eigenvectors with nonzero eigenvalues. It is reasonable to do so. By inserting Eq. (B9) into Eq. (B3), we rewrite $\mathcal{F}_\lambda$ as

$$
\mathcal{F}_\lambda = \boldsymbol{b}^{\mathrm{T}}\mathcal{M}\boldsymbol{b}. \tag{B12}
$$

Suppose $\mathcal{M}$ has spectral decomposition

$$
\mathcal{M} = \sum_{i=1}^{d^2-1} m_i \boldsymbol{v}_i \boldsymbol{v}_i^{\mathrm{T}}, \tag{B13}
$$

where $\boldsymbol{v}_i$ denotes an eigenvector with eigenvalue $m_i$. We assume $m_i \neq 0$ for $i = 1,\ldots,n$ and $m_i = 0$ for $i = n+1,\ldots,d^2 - 1$. With Eq. (B13), Eq. (B12) reads

$$
\mathcal{F}_\lambda = \sum_{i=1}^{n} m_i \boldsymbol{b}^{\mathrm{T}}\boldsymbol{v}_i\boldsymbol{v}_i^{\mathrm{T}}\boldsymbol{b}. \tag{B14}
$$

It is shown that $\mathcal{F}_\lambda$ is defined on suppl($\mathcal{M}$).

## APPENDIX C: DERIVATION OF EQ. (66)

In this Appendix, we give the detailed derivation of $\mathcal{I}_\lambda$ in terms of the Bloch vector for mixed states given by Eq. (66). We first expand the Hermitian matrix as

$$
\sqrt{\rho} = y\mathbb{1}_d + \boldsymbol{x}\cdot\hat{\boldsymbol{\eta}}, \tag{C1}
$$

where $y = \mathrm{Tr}(\sqrt{\rho})/d$ and $\boldsymbol{x}$ is an unknown $(d^2 - 1)$-dimensional real vector. With Eq. (C1), $\mathcal{I}_\lambda$ in Eq. (16) can be rewritten as

$$
\mathcal{I}_\lambda = 8\left[ (\partial_\lambda y)^2 + \frac{2}{d}|\partial_\lambda\boldsymbol{x}|^2 \right] \tag{C2}
$$

by using the properties of the generators of the Lie algebra given in Appendix A. Furthermore, we have the following equation:

$$
\rho = (\sqrt{\rho})^2. \tag{C3}
$$

In the Bloch representation, the left-hand side of the equation above is given by Eq. (55), and the right-hand side reads

$$
(\sqrt{\rho})^2 = \left( y^2 + \frac{2}{d}|\boldsymbol{x}|^2 \right)\mathbb{1}_{d^2-1} + \sum_k (2yx_k + g_{ijk}x_i x_j)\hat{\eta}_k.
$$

By comparing the terms on both sides, one finds that $y$ and $\boldsymbol{x}$ are completely determined by the following $d^2$ quadratic nonlinear equations:

$$
y^2 + \frac{2}{d}|\boldsymbol{x}|^2 = \frac{1}{d}, \tag{C4}
$$

$$
\sum_{i,j=1}^{d^2-1} g_{ijk}x_i x_j + 2yx_k = \frac{\omega_k}{2} \tag{C5}
$$

for $k = 1,2,\ldots,d^2 - 1$.

Below, we give the detailed derivation for Eqs. (71) and (72). Multiplying the LHS of Eq. (70) by $4y\boldsymbol{x}^{\mathrm{T}}$ and the RHS by $\boldsymbol{\omega}^{\mathrm{T}}$, we obtain

$$
16y^2|\boldsymbol{x}|^2 = |\boldsymbol{\omega}|^2. \tag{C6}
$$

By replacing $|\boldsymbol{x}|^2$ in the equation above by

$$
|\boldsymbol{x}|^2 = \tfrac{1}{2} - y^2, \tag{C7}
$$

given by Eq. (69), we get the following equation:

$$
16y^4 - 8y^2 + |\boldsymbol{\omega}|^2 = 0. \tag{C8}
$$

Solving the above equation, we obtain two solutions,

$$y_+^2 = \frac{1 + \sqrt{1 - |\boldsymbol{\omega}|^2}}{4}, \tag{C9}$$

$$y_-^2 = \frac{1 - \sqrt{1 - |\boldsymbol{\omega}|^2}}{4}. \tag{C10}$$

We suppose that $\rho$ has spectral decomposition

$$\rho = \sum_i \varrho_i |\psi_i\rangle\langle\psi_i| = \varrho_1 |\psi_1\rangle\langle\psi_1| + (1 - \varrho_1)|\psi_2\rangle\langle\psi_2|. \tag{C11}$$

Then we can derive the following inequality:

$$y = \frac{1}{2}\mathrm{Tr}\left(\sqrt{\rho}\right) = \frac{1}{2}\sum_i \sqrt{\varrho_i} \geqslant \frac{1}{2}. \tag{C12}$$

Then the solution $y_-^2$ in Eq. (C10) can be neglected. Due to $y$ being a non-negative real number, we finally get Eq. (71) from Eq. (C9). Furthermore, substituting Eq. (71) into Eq. (70) directly yields Eq. (72).

### APPENDIX D: DERIVATION OF THE AFFINE TRANSFORMATION MATRIX $A$ AND $c$ FOR THE COLLISIONAL DEPHASING

We first verify that the elements of the Bloch vector can be directly written out from the elements of the density matrix. A $d$-dimensional density matrix is described by the generalized Bloch vector in Eq. (55) in the Bloch representation. The elements of the generalized Bloch vector are defined by

$$\omega_i = \mathrm{Tr}\left(\rho\,\hat{\eta}_i\right). \tag{D1}$$

In Appendix A, we systematically construct the generators of Lie algebra su $(d)$ in Eq. (A13), which is defined by three sets given by Eqs. (A9), (A10), and (A11). Then $\boldsymbol{\omega}$ also can be divided into three parts as

$$\{\omega_i\}_{i=1}^{d^2-1} = \left\{\omega_{m,n}^{\mathcal{S}}, \omega_{m,n}^{\mathcal{A}}, \omega_k^{\mathcal{D}}\right\}. \tag{D2}$$

We find that the elements of the Bloch vector are directly given by the elements of the density matrix,

$$\omega_{m,n}^{\mathcal{S}} = \mathrm{Tr}\left(\rho\,\hat{\mathcal{S}}_{m,n}\right) = 2\,\mathrm{Re}\left(\rho_{m,n}\right), \tag{D3}$$

$$\omega_{m,n}^{\mathcal{A}} = \mathrm{Tr}\left(\rho\,\hat{\mathcal{A}}_{m,n}\right) = -2\,\mathrm{Im}(\rho_{m,n}), \tag{D4}$$

$$\omega_k^{\mathcal{D}} = \mathrm{Tr}\left(\rho\,\hat{\mathcal{D}}_k\right) = \sqrt{\frac{2}{k\,(k+1)}}\left[\sum_{m=1}^{k}\rho_{m,m} - k\,\rho_{k+1,k+1}\right]. \tag{D5}$$

The master equation of the collisional dephasing model is described by Eq. (82), and the time evolution of the density-matrix elements is given by Eq. (84). With Eqs. (84), (D3), (D4), and (D3), the elements of the affine-mapped Bloch vector are given by

$$\omega_{m,n}^{\mathcal{S}}(t) = e^{-(m-n)^2\tau}\,2\,\mathrm{Re}\left[\rho_{m,n}(0)\right] = e^{-(m-n)^2\tau}\omega_{m,n}^{\mathcal{S}}(0), \tag{D6}$$

$$\omega_{m,n}^{\mathcal{A}}(t) = -e^{-(m-n)^2\tau}\,2\,\mathrm{Im}\left[\rho_{m,n}(0)\right] = e^{-(m-n)^2\tau}\omega_{m,n}^{\mathcal{A}}(0), \tag{D7}$$

$$\omega_k^{\mathcal{D}}(t) = \omega_k^{\mathcal{D}}(0). \tag{D8}$$

Equation (D8) illustrates that $\boldsymbol{\omega}_k^{\mathcal{D}}$ remains unchanged under the collisional dephasing, since $\boldsymbol{\omega}_k^{\mathcal{D}}$ depends on the diagonal elements of the density matrix which are left unchanged by dephasing. Writing in the form of an affine map in Eq. (74), we finally obtain $A$ in Eq. (85) and $c = 0$ from Eqs. (D6), (D7), and (D8).

[1] D. Petz, Linear Alegbra Appl. **244**, 81 (1996).

[2] L. Pezzé and A. Smerzi, Phys. Rev. Lett. **102**, 100401 (2009).

[3] J. Ma and X. G. Wang, Phys. Rev. A **80**, 012318 (2009).

[4] Á. Rivas and A. Luis, Phys. Rev. Lett. **105**, 010403 (2010).

[5] Z. Sun, J. Ma, X. M. Lu, and X. G. Wang, Phys. Rev. A **82**, 022306 (2010).

[6] J. Ma, Y. X. Huang, X. G. Wang, and C. P. Sun, Phys. Rev. A **84**, 022302 (2011).

[7] R. Chaves, L. Aolita, and A. Acín, Phys. Rev. A **86**, 020301(R) (2012).

[8] J. Ma, X. G. Wang, C. P. Sun, and F. Nori, Phys. Rep. **509**, 89 (2011).

[9] P. Hyllus, W. Laskowski, R. Krischek, C. Schwemmer, W. Wieczorek, H. Weinfurter, L. Pezzé, and A. Smerzi, Phys. Rev. A **85**, 022321 (2012).

[10] G. Tóth, Phys. Rev. A **85**, 022322 (2012).

[11] V. Giovannetti, S. Lloyd, and L. Maccone, Phys. Rev. Lett. **96**, 010401 (2006).

[12] V. Giovannetti, S. Lloyd, and L. Maccone, Nat. Photon. **5**, 222 (2011).

[13] S. F. Huelga, C. Macchiavello, T. Pellizzari, A. K. Ekert, M. B. Plenio, and J. I. Cirac, Phys. Rev. Lett. **79**, 3865 (1997).

[14] R. Chaves, J. B. Brask, M. Markiewicz, J. Kołodyński, and A. Acín, e-print arXiv:1212.3286.

[15] B. M. Escher, R. L. de Matos Fillo, and L. Davidovich, Nat. Phys. **7**, 406 (2011).

[16] R. Demkowicz-Dobrzański, J. Kołodyński, and M. Gută, Nat. Commun. **3**, 1063 (2012).

[17] H. Uys and P. Meystre, Phys. Rev. A **76**, 013804 (2007).

[18] A. Shaji and C. M. Caves, Phys. Rev. A **76**, 032111 (2007).

[19] S. Boixo, A. Datta, M. J. Davis, S. T. Flammia, A. Shaji, and C. M. Caves, Phys. Rev. Lett. **101**, 040403 (2008).

[20] S. M. Roy and S. L. Braunstein, Phys. Rev. Lett. **100**, 220501 (2008).

[21] M. G. A. Pairs, Int. J. Quantum Inform. **7**, 125 (2009).

[22] Y. C. Liu, Z. F. Xu, G. R. Jin, and L. You, Phys. Rev. Lett. **107**, 013601 (2011).

[23] J. Joo, W. J. Munro, and T. P. Spiller, Phys. Rev. Lett. **107**, 083601 (2011).

[24] D. W. Berry, M. J. W. Hall, M. Zwierz, and H. M. Wiseman, Phys. Rev. A **86**, 053813 (2012).

[25] M. J. W. Hall and H. M. Wiseman, Phys. Rev. X **2**, 041006 (2012).

[26] M. Tsang, Phys. Rev. Lett. **108**, 230401 (2012).

[27] C. W. Helstrom, *Quantum Detection and Estimation Theory* (Academic, New York, 1976).

[28] A. S. Holevo, *Probabilistic and Statistical Aspects of Quantum Theory* (North-Holland, Amsterdam, 1982).

[29] W. K. Wootters, Phys. Rev. D **23**, 357 (1981).

[30] S. L. Braunstein and C. M. Caves, Phys. Rev. Lett. **72**, 3439 (1994).

[31] X. M. Lu, X. G. Wang, and C. P. Sun, Phys. Rev. A **82**, 042103 (2010).

[32] E. P. Wigner and M. M. Yanase, Proc. Natl. Acad. Sci. USA **49**, 910 (1963).

[33] S. L. Luo, Phys. Rev. A **73**, 022324 (2006).

[34] S. L. Luo, S. S. Fu, and C. H. Oh, Phys. Rev. A **85**, 032117 (2012).

[35] K. M. R. Audenaert, J. Calsamiglia, R. Muñoz-Tapia, E. Bagan, Ll. Masanes, A. Acin, and F. Verstraete, Phys. Rev. Lett. **98**, 160501 (2007).

[36] J. Calsamiglia, R. Muñoz-Tapia, Ll. Masanes, A. Acin, and E. Bagan, Phys. Rev. A **77**, 032311 (2008).

[37] W. Forrest Stinespring, Proc. Amer. Math. Soc. **6**, 211 (1955).

[38] K. Kraus, Ann. Phys. (NY) **64**, 311 (1971).

[39] P. Gibilisco and T. Isola, J. Math. Phys. **44**, 3752 (2003).

[40] M. A. Nielsen and I. L. Chuang, *Quantum Computation and Quantum Information* (Cambridge University Press, Cambridge, 2010).

[41] X. G. Wang, A. Miranowicz, Y. X. Liu, C. P. Sun, and F. Nori, Phys. Rev. A **81**, 022106 (2010).

[42] M. Bartkowiak, A. Miranowicz, X. G. Wang, Y. X. Liu, W. Leoński, and F. Nori, Phys. Rev. A **83**, 053814 (2011).

[43] L. Aolita, R. Chaves, D. Cavalcanti, A. Acín, and L. Davidovich, Phys. Rev. Lett. **100**, 080501 (2008).

[44] H. P. Breuer and F. Petruccione, *The Theory of Open Quantum Systems* (Oxford University Press, Oxford, 2007).

[45] V. Gorini, A. Kossakowski, and E. C. G. Sudarshan, J. Math. Phys. **17**, 821 (1976).

[46] Y. Yan, F. Yang, Y. Liu, and J. Shao, Chem. Phys. Lett. **395**, 216 (2004); Y. Zhou, Y. Yan, and J. Shao, Europhys. Lett. **72**, 334 (2005); H. Li, J. Shao, and S. Wang, Phys. Rev. E **84**, 051112 (2011).

[47] R. X. Xu, P. Cui, X. Q. Li, Y. Mo, and Y. J. Yan, J. Chem. Phys. **122**, 041103 (2004); R. X. Xu and Y. J. Yan, Phys. Rev. E **75**, 031107 (2007); J. Xu, R. X. Xu, and Y. J. Yan,

[48] Y. Tanimura and R. Kubo, J. Phys. Soc. Jpn. **58**, 101 (1989); Y. Tanimura, Phys. Rev. A **41**, 6676 (1990); Y. Tanimura and P. G. Wolynes, *ibid.* **43**, 4131 (1991).

[49] Y. Tanimura, J. Phys. Soc. Jpn. **75**, 082001 (2006).

[50] A. Ishizaki and Y. Tanimura, J. Phys. Soc. Jpn. **74**, 3131 (2005); J. Chem. Phys. **125**, 084501 (2006); J. Phys. Chem. A **111**, 9269 (2007).

[51] A. Ishizaki and G. R. Fleming, Proc. Natl. Acad. Sci. (USA) **106**, 17255 (2009); M. Sarovar, A. Ishizaki, G. R. Fleming, and K. B. Whaley, Nat. Phys. **6**, 462 (2010).

[52] J. Ma, Z. Sun, X. G. Wang, and F. Nori, Phys. Rev. A **85**, 062323 (2012).

[53] X. L. Yin, J. Ma, X. G. Wang, and F. Nori, Phys. Rev. A **86**, 012308 (2012).

[54] R. A. Fisher, Proc. Cambridge Philos. Soc. **22**, 700 (1925).

[55] D. Bures, Trans. Amer. Math. Soc. **135**, 199 (1969).

[56] A. Uhlmann, Rep. Math. Phys. **9**, 273 (1976).

[57] M. Hübner, Phys. Lett. A **163**, 239 (1992).

[58] S. L. Luo and Q. Zhang, Phys. Rev. A **69**, 032106 (2004).

[59] J. Dittmann, J. Phys. A **32**, 2663 (1999).

[60] S. L. Luo, Phys. Rev. Lett. **91**, 180403 (2003).

[61] Y. Watanabe, T. Sagawa, and M. Ueda, Phys. Rev. Lett. **104**, 020401 (2010).

[62] K. Lendi, J. Phys. A **20**, 15 (1987).

[63] R. Alicki and K. Lendi, *Quantum Dynamical Semigroups and Applications*, Lecture Notes in Physics Vol. 717 (Springer, Berlin, 2007).

[64] X. G. Wang and B. C. Sanders, Phys. Rev. A **68**, 012101 (2003).

[65] S. Boixo, A. Datta, M. J. Davis, A. Shaji, A. B. Tacla, and C. M. Caves, Phys. Rev. A **80**, 032103 (2009).

[66] N. Bar-Gill, D. D. Bhaktavatsala Rao, and G. Kurizki, Phys. Rev. Lett. **107**, 010404 (2011).

[67] Y. C. Liu, G. R. Jin, and L. You, Phys. Rev. A **82**, 045601 (2010).

[68] Y. Khodorkovsky, G. Kurizki, and A. Vardi, Phys. Rev. A **80**, 023609 (2009).

[69] U. Dorner, New J. Phys. **14**, 043011 (2012).